ICAS-96-2.7.3

AERODYNAMIC SHAPE OPTIMIZATION BASED ON HIGH-LEVEL PHYSICS

K. D. Lee and S. Eyi
Aeronautical and Astronautical Engineering
University of Illinois,
Urbana, Illinois 61801, U. S. A.

Abstract

This paper presents an aerodynamic design method that is based on computational fluid dynamics and numerical optimization. The flow was modeled with high-level physics in order to produce reliable designs. Constrained optimization was used to achieve the design objective without degenerating other performance characteristics. Flow sensitivities were evaluated by finite differencing due to its simplicity. One merit of the approach is that it does not require any new tools. It utilizes existing well-validated tools for flow analysis, grid generation, and optimization. The paper also discusses some design issues associated with the efficiency of the design process. Results were presented for transonic drag reduction, multi-point design, and single- and multi-element high-lift designs.

Introduction

Advances in computer and computational techniques have changed the aerodynamic design process.[1] Computational fluid dynamics (CFD) has emerged as an efficient design tool due to its ability to provide detailed flowfield information on many geometries in a short period of time at modest cost. It can reduce engineering interactions to achieve a design goal and hence shorten overall engineering effort and calendar time for a development. One of the early CFD design applications was based on the cut-and-try approach where a designer iteratively modifies and verifies a design. This method is expensive and time-consuming, and requires considerable expertise to produce a successful design. Performing such a design method with wind-tunnel models would be even more costly. In the approach, an improvement in one aspect of performance can easily accompany undesirable changes in other aspects, especially when the design process involves a large number of design variables on a complex design space.

Numerical optimization is an improvement over the cut-and-try approach because it is based on a rational, directed, design procedure. It generates an optimum geometry that improves aerodynamic performance characteristics while satisfying specified design constraints. One example is drag minimization without reducing the lift and thickness of an airfoil. Constrained optimization is attractive because it can achieve multiple design objectives, impose multiple design constraints, and perform multi-point designs. The use of optimization in aerodynamic design is not new,[2-4] but in the past its applications were limited by computing power and cost. The interest in design optimization has been renewed[5-8] as the rapidly-advancing computer technology brought in a new engineering environment. Now CFD-based design optimization is becoming more practical and affordable.

This paper presents a CFD-based design method and discusses some issues associated with the reliability and efficiency of the design process. It also discusses results of several design practices in transonic drag reduction, multi-point design, and high-lift design.

Method

The present design method utilizes a numerical optimizer[9] to drive a flow analysis code to find a geometry that minimizes an objective function while satisfying specified constraints. Both the objective function and constraints are functions of aerodynamic performance parameters. In order to form a minimization problem, they are defined as percent changes from their initial values into the favorable direction. One design cycle consists of four steps: analysis, sensitivity, optimization, and geometry modification. The analysis step evaluates the values of the objective and constraint functions, and the sensitivity step finds their derivatives with respect to design variables. In shape optimization, design variables are geometry perturbations, and hence sensitivities are the responses of the flow to geometry perturbations.

The optimization step finds the values of design variables that minimize the objective function, and the modification step changes the geometry and generates the grid around it.

While the optimization algorithm determines the convergence of a design cycle, the reliability of a design method depends on the ability to produce accurate flow solutions. Therefore, the flow model used in design should be able to represent all of the significant flow physics involved. For example, transonic designs require a flow model of high-level physics such as the Euler or Navier-Stokes equations to represent the rotational flow physics involving shock waves. Also, the grid should be fine enough to accommodate the length scales of the flow physics. Refined grids are needed in regions of large flow gradients as in boundary layers and near shocks. A surface-fitted coordinate system was used in the present study to facilitate the implementation of boundary conditions.

There are two approaches in evaluating sensitivities: analytical and finite-difference. The analytical approach is advantageous because it produces accurate sensitivities and is cost efficient. It can also employ the adjoint equation formulation,[8-10] which makes the sensitivity evaluation cost virtually independent of the number of design variables. However, it requires a sensitivity code for each analysis code used. Meanwhile, the finite-difference approach does not require the sensitivity code and is simple to use. It is expensive because it requires an analysis per design variable per design cycle, especially when the number of design variables is large. It also has accuracy problems due to truncation and condition errors. However, the efficiency of finite-difference sensitivities can be improved through a careful implementation.[11-12] In the present study, sensitivities were obtained by a finite difference approach.

In addition to the optimization algorithm and the flow code, another factor that influences the performance and efficiency of a design process is the choice of base functions. The perturbation to be added to the initial geometry is defined as a linear combination of base functions. Any smoothly distributed curves over the airfoil chord can be used as the base functions. The accuracy and efficiency of a design process depends on the number and shape of the base functions. The use of too few base functions cannot produce a satisfactory design, and too many base functions increase the design cost without improving the design. Some base functions may cause wavy geometry perturbations, and hence result in wavy pressure distributions, which sometimes slow down or destroy the convergence of the design cycle. In the present study, the Hicks-Henne functions[13] were used as base functions.

Another issue in design optimization is that the optimization process may find a locally optimum solution instead of finding a globally optimum design. This drawback is especially important when the design is performed using high-level flow models and the flow field involves complex nonlinear flow physics such as shock/boundary-layer interactions and flow separations. With no clear means of avoiding local minimums, the present study handled this issue with the choice of base geometry and side constraints limiting the variation of design variables.

Transonic Drag Reduction

Transonic flow involves embedded shock waves and shock-boundary-layer interactions that are difficult to predict with low-level flow models. The objective in the present transonic airfoil design is to reduce total transonic drag. Constraints are needed on the lift and the airfoil cross-sectional area, so that these values are not decreased. The area constraint was chosen over the thickness constraint because the former is easier to enforce. Transonic drag reduction was attempted for the RAE 2822 airfoil at the Case 9 flow condition of the AGARD experimental data base ($M= 0.730$, $\alpha=2.78^{o}$, $Re=6.5x10^{6}$). Three different flow models were used: Euler on an Euler grid, Navier-Stokes on a coarse grid, and Navier-Stokes on a fine grid. The grid size was 129x33 for Euler, 129x49 for Navier-Stokes-coarse, and 257x65 for Navier-Stokes-fine. The near-field grids are shown in Figure 1. Ten base functions were used to modify the geometry.

Design optimizations were performed using different flow physics, and the resulting airfoils were evaluated using the Navier-Stokes-fine analysis to analyze the design performance. Table 1 and Figure 2 show the results. The Euler design produced a significant reduction in Euler drag at a lower cost. However, when the designed airfoil was analyzed using Navier-Stokes-fine analysis, there was only a minimal drag reduction. Also it was accompanied by a loss of lift and the formation of an undesirable double-shock structure, as seen in Figure 2a. The double-shock will thicken the boundary layer that cannot be predicted by the Euler physics. For the design using the Navier-Stokes-coarse model, there was a reasonable drag reduction, the lift constraint was satisfied, and no double-shock was formed. When this design was

analyzed with Navier-Stokes-fine, there was a rather larger drag reduction than predicted by the design. The design using Navier-Stokes-fine may produce the most reliable result but cost four-times as much CPU time than the Navier-Stokes-coarse design. This study indicates that the Navier-Stokes-coarse design was the most efficient from the design-quality and design-cost viewpoint. Although the Euler design is economically attractive, it is not useful when actual flight performance of the design is considered. Another issue is that all the designs obtained are locally optimum solutions with no guarantee that a globally optimum solution was reached.

Two-Point Design

A major limitation of single-point design is poor off-design-point performance. The objective of multi-point design is to improve overall performance of a design over a flight envelope. Two-point design was performed to obtain an airfoil geometry which produces minimum transonic drag at two flight conditions: the primary design-point and the secondary design-point. This was achieved subject to inequality constraints on the lift at the primary design-point and the airfoil area, so that these values are not decreased by the optimized airfoil. All designs were performed on the RAE 2822 airfoil using a 129x33 grid. The flow was modeled by the Euler physics and a total of sixteen design variables were used. The primary design-point flow condition was selected to be Case 6 of the AGARD experimental data base (M=0.726, α=2.44^o) and the secondary point was chosen at different Mach number or angle-of-attack.[14]

Figure 3 shows the aerodynamic characteristics for the single-point and two two-point design cases with the angle-of-attack variation for the secondary design-point. Several designs were performed to evaluate the effect of the weighting parameter, w, between the primary and secondary design points. The main advantage of two-point design can be seen in Figure 4. The single-point design has a large drag creep that begins immediately away from the primary design-point. The w=0.50 two-point design removes this drag creep, but at the expense of a reduced drag-reduction at the primary design-point. The w=0.70 two-point design represents a compromise: large reduced drag at the primary design-point and a small reduced drag at the secondary design-point. Figure 5 shows the drag reduction at the two design-points as a function of the weighting parameter and demonstrates a nonlinear effect of the weighting parameter.

High-Lift Design

High-lift aerodynamics is one of the pending items in the development of future transport aircraft. High-lift systems involve both complex geometry and complex flow physics. They are usually composed of multiple elements, such as leading-edge slats and multiple slotted flaps, and include challenging flow physics such as turbulent flow, separation, transition, and confluent boundary-layer wakes. In the present study, high-lift designs were performed based on the incompressible Navier-Stokes equations using the INS2D computer code.[15] High-lift designs[16] were performed for both single- and multi-element airfoils. The chimera overset grid system[17] was used to discretize the flow field around a multi-element airfoil. Figures 6 and 7 show the grid system around multi- and single-element airfoils respectively.

A single-element high-lift design was performed with the NACA 4412 airfoil at angles of attack of 16 degrees which is a stalling condition. The Reynolds number was set to 1.5 million and the grid size was 241x61. The airfoil geometry was modified by using fourteen Hicks-Henne functions. Constraints were imposed on the drag and the airfoil cross-sectional area. Table 2 and Figure 8 show design results. The design required 139 function calls with total iterations equivalent to 33 analyses. An interesting observation is that the optimization made a flap out of the aft portion of the airfoil, resulting in a large increase of lift and a substantial reduction in drag. The separated flow region was reduced in the designed airfoil as shown in Figure 9.

A multi-element high-lift design was demonstrated for a three-element airfoil at take-off and landing configurations. The grid system was composed of four grids; three C-grids around the slat, main element, and flap, and an H-grid for the flap wake. The grid sizes were 121x31, 281x85, 121x41, and 21x37 respectively with a total of 33374 grid points. The optimization was performed at angles of attack of 8.10 and 16.21 degrees and a Reynolds number of 9 million. The design variables used were relative positions between multiple elements; gap, rotation, and overhang. The geometry of each element was kept unchanged. Results are shown in Table 3 and Figure 10. Both designs produced a substantial gain in lift and reduction in drag at a relatively low cost. The α=8.10^o design required 14 function calls with a total of 1993 iterations and the α=16.21^o design required 20 function calls with a total of 2917

iterations. With the same grid, one analysis for converged solutions took 223 and 732 iterations for $\alpha=8.10^{\circ}$ and $\alpha=16.21^{\circ}$ respectively. One flow iteration cost .76 CPU seconds on Cray C-90. Unlike single-element airfoil optimization, multi-element airfoil design optimization required strict side constraints on the design variables in order to account for the limitations imposed on the geometry and the relative position of airfoil elements.

Concluding Remarks

An aerodynamic shape optimization method was used to perform several designs: transonic drag reduction, multi-point design, and high-lift design. Those design practices provided valuable lessons and also raised important issues. High-level flow physics should be used to obtain reliable designs, but the use of excessively refined flow models merely increases design cost without improving the quality of design results. Sensitivity evaluation by Finite-differencing is expensive but still useful in certain applications when the number of design variables is small. The performance of a design process depends on parameters such as the initial condition, the choice and number of design variables, the number and tolerance of constraints, the accuracy of sensitivities, the cost of sensitivity analysis, etc. and therefore can be improved through a careful implementation. Optimization-driven design methods are becoming more and more affordable in the current computing environment and will enhance the whole aircraft manufacturing process in the future.

References

1. Rubbert, P. E., "CFD and the Changing World of Aircraft Design," AIAA Wright Brothers Lecture, Anaheim, CA, Sept. 1994.
2. Hicks, R. M., Murman, E. M. and Vanderplaats, G. N., "An Assessment of Aerofoil Design by Numerical Optimization", NASA TM X-3092, 1974.
3. Hicks, R. M. and Henne, P. A., "Wing Design by Numerical Optimization," Journal of Aircraft, Vol. 15, No. 7, July 1978, pp. 407-412.
4. Mani, K. K., "Design Using Euler Equations", AIAA Paper 84-2166, AIAA 2nd Applied Aerodynamic Conference, Seattle, WA, August 1984.
5. Lee, K. D. and Eyi, S., "Aerodynamic Design Via Optimization," Journal of Aircraft, Vol. 29, No. 6, pp. 1012-1019, Nov.-Dec. 1992.
6. Eyi, S., Hager, J. O., and Lee, K. D., "Airfoil Design Optimization Using the Navier-Stokes Equations," Journal of Optimization Theory and Applications, Vol. 83, No. 3, pp. 447-461, Dec. 1994.
7. Jameson, A., "Aerodynamic Theory via Control Theory," Journal of Scientific Computing, Vol. 3, pp. 233-260, 1988.
8. Reuther, J. and Jameson, A., "Aerodynamic Shape Optimization of Wing and Wing-Body Configurations Using Control Theory," AIAA Paper 95-0123, Reno, NV, Jan. 1995.
9. Vanderplaats, G. N. and Hansen S. R., "DOT Users Manual," VMA Engineering, Goleta, CA, 1989.
10. Baysal, O. and Elashaky, M. E., "Aerodynamic Sensitivity Analysis Methods for the Compressible Euler Equations," Journal of Fluid Engineering, 113(4), pp. 681-688, 1991.
11. Eyi, S. and Lee, K. D., "Effects of Sensitivity Analysis on Aerodynamic Design Optimization," Proceedings of Forum on Computational Fluid Dynamics for Design and Optimization, pp. 1-8, San Francisco, CA, Nov. 1995.
12. Eyi, S. and Lee, K. D., "Efficiency Improvement of Sensitivity Evaluation for Aerodynamic Shape Optimization," AIAA Paper 96-2506, Proceedings of 14th Applied Aerodynamic Conference, New Orleans, LA, June 1996.
13. Hicks, R. M. and Henne, P. A., "Wing Design by Numerical Optimization," Journal of Aircraft, Vol. 15, No. 7, July 1978, pp. 407-412.
14. Hager, J. O., Eyi, S., and Lee, K. D., "Two-Point Transonic Airfoil Design Using Optimization for Improved Off-Design Performance," Journal of Aircraft, Vol. 31, No. 6, pp. 1143-1147, Nov.-Dec. 1994.
15 Rogers, S. E., Wiltberger, N. L., and Kwak, D., "Efficient Simulation of Incompressible Viscous Flow Over Single and Multi-Element Airfoils," AIAA Paper 92-0405, AIAA 30th Aerospace Sciences Meeting and Exhibit, Reno, NV, January 1992.
16. Eyi, S., Lee, K. D., Rogers, S. E., and Kwak, D., "High-Lift Design Optimization Using the Navier-Stokes Equations," AIAA Paper 95-0477, AIAA 33rd Aerospace Sciences Meeting, Reno, NV, Jan. 1995.
17. Benek, J. A., Buning, P. G., and Steger J. L., "A 3-D Chimera Grid Embedding Technique," AIAA Paper 85-1523-CP, July 1985.

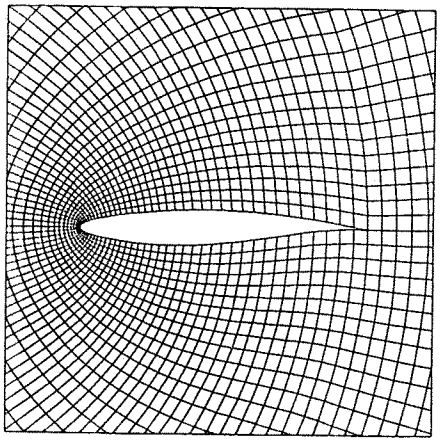

(a) Euler grid (129x33, 96 on surface)

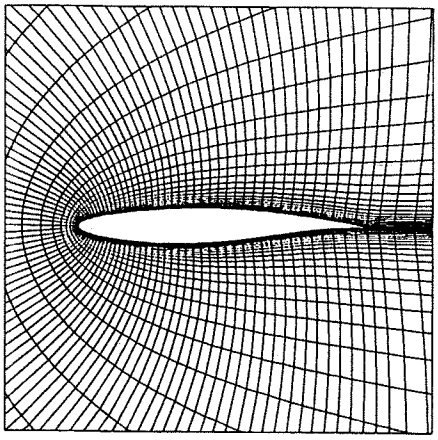

(b) N-S coarse grid (129x49, 96 on surface)

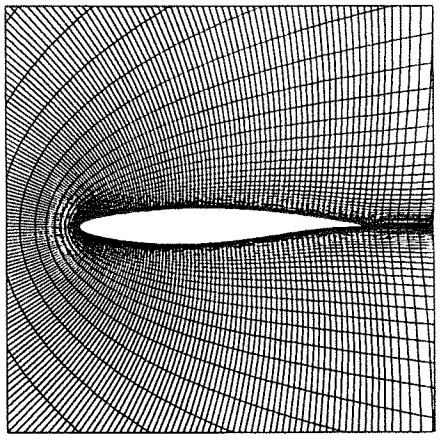

(c) N-S fine grid (257x65, 192 on surface)

Figure 1. Close view of the RAE 2822 grids.

Table 1. Aerodynamic characteristic results for minimum-drag design of the RAE 2822 airfoil with lift and area constraints at Case 9.
($M=0.730$, $\alpha=2.78°$, $Re=6.5\times10^6$)

(a) Euler design.

		Initial	Final	Δ	Δ (%)
Euler	C_l	0.9360	0.9351	-0.0008	-0.09
Design	C_d	0.0197	0.0100	-0.0097	-49.34
	C_m	-0.1315	-0.1185	0.0129	-9.82
N/S	C_l	0.8000	0.7448	-0.0552	-6.90
Fine	C_d	0.0200	0.0197	-0.0002	-1.24
Anal.	C_m	-0.0990	-0.0969	0.0021	-2.13
	A	0.0780	0.0780	0.0000	0.00

$N_{geom} = 44$, $T = 0.27$, $E = 0.58$

(b) Navier-Stokes-coarse design.

		Initial	Final	Δ	Δ (%)
N/S	C_l	0.7937	0.7832	-0.0104	-1.31
Coarse	C_d	0.0222	0.0200	-0.0022	-9.73
Design	C_m	-0.1014	-0.0984	0.0030	-2.94
N/S	C_l	0.8000	0.8006	0.0006	0.07
Fine	C_d	0.0200	0.0165	-0.0035	-17.40
Anal.	C_m	-0.0990	-0.0947	0.0044	-4.44
	A	0.0780	0.0780	0.0000	0.00

$N_{geom} = 35$, $T = 1.33$, $E = 1.66$

(c) Navier-Stokes-fine design.

		Initial	Final	Δ	Δ (%)
Design	C_l	0.8000	0.7811	-0.0190	-2.37
and	C_d	0.0200	0.0174	-0.0026	-13.16
Anal.	C_m	-0.0990	-0.0953	0.0038	-3.82
	A	0.0780	0.0780	0.0000	0.00

$N_{geom} = 49$, $T = 5.68$, $E = 0.29$

A = cross-sectional area of the airfoil
N_{geom} = number of geometries evaluated
T = design (CPU) time, scaled using N-S-coarse design value
E = efficiency = $\Delta C_d / T$, scaled using N-S-coarse design value

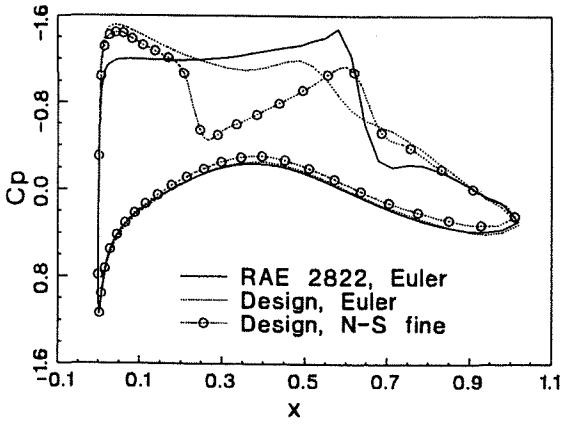

(a) Euler design surface pressure comparison

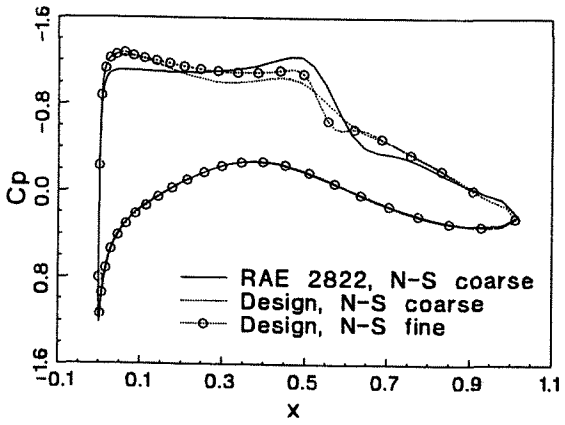

(b) Navier-Stokes-coarse design surface pressure comparison

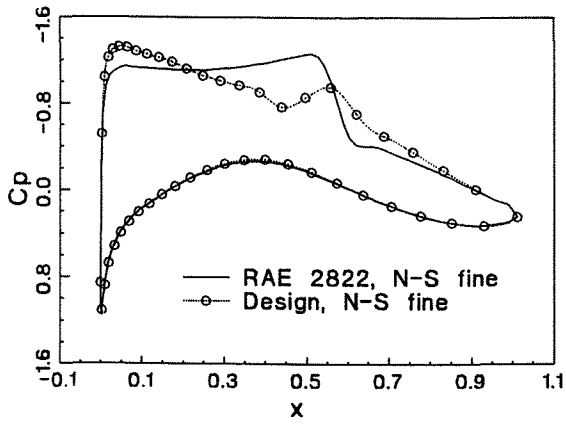

(c) Navier-Stokes-fine design surface pressure comparison

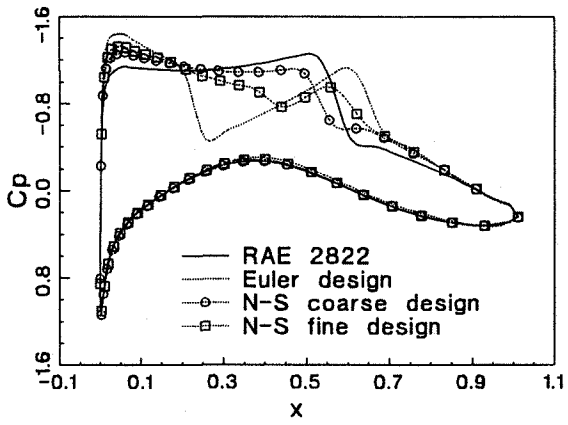

(d) Surface pressure comparison for all designs using Navier-Stokes fine analysis

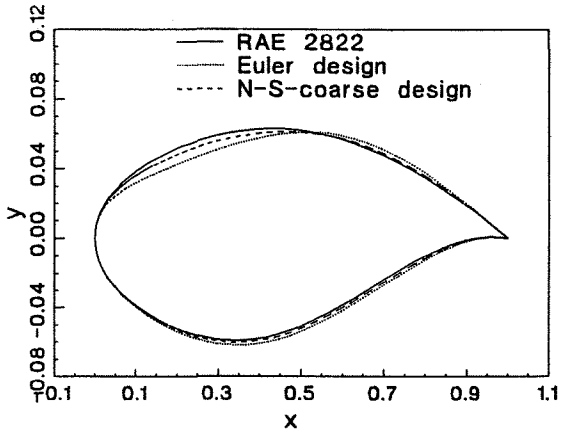

(e) Airfoil geometry comparison for the Euler and Navier-Stokes-coarse designs

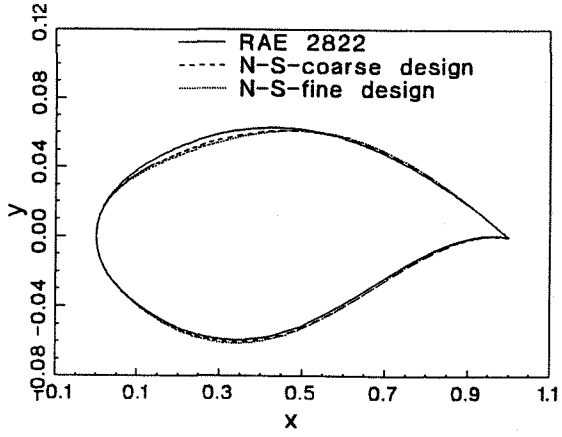

(f) Airfoil geometry comparison for the N-S-coarse and N-S fine designs

Figure 2. Results for minimum-drag design of the RAE 2822 airfoil with lift and area constraint at Case 9. ($M = 0.730$, $\alpha = 2.78^{\circ}$, $Re = 6.5 \times 10^{6}$)

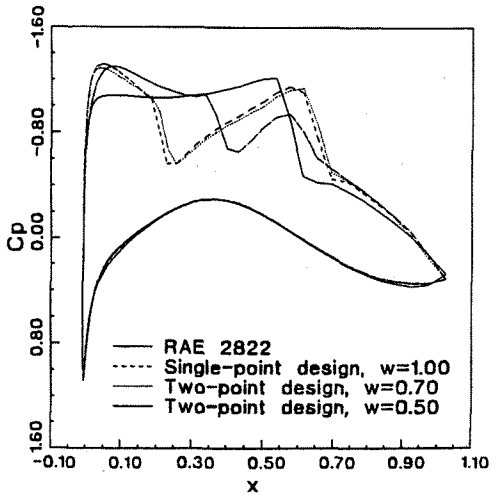

(a) Surface pressure comparison at condition 1

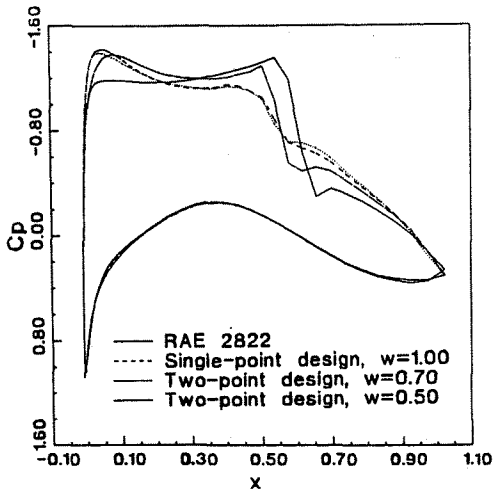

(b) Surface pressure comparison at condition 2

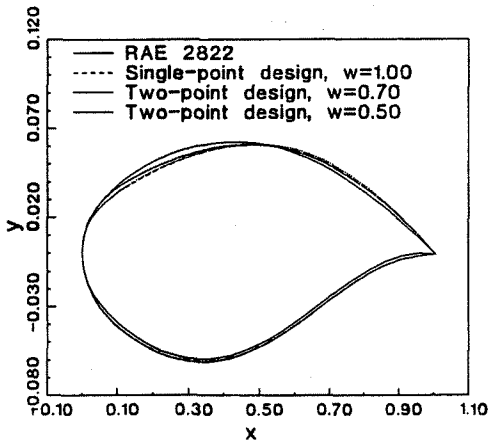

(c) Airfoil geometry comparison

Figure 3. RAE 2822 alpha-design results.
($M_1 = 0.726$, $\alpha_1 = 2.44^\circ$)
($M_2 = 0.726$, $\alpha_2 = 2.00^\circ$)

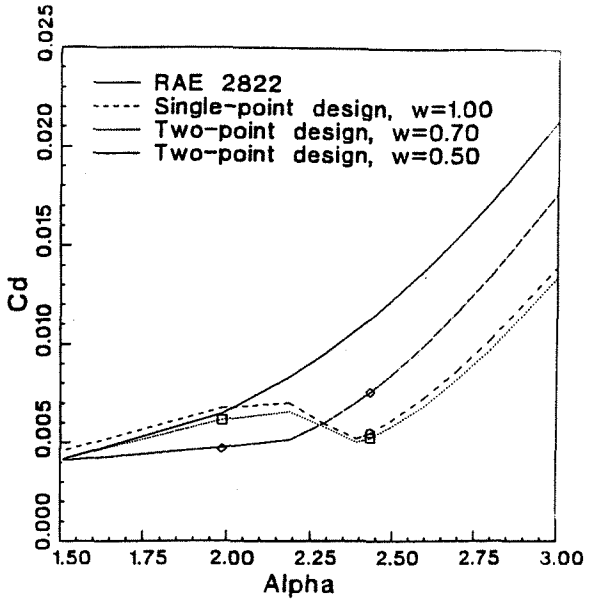

Figure 4. RAE 2822 alpha-design, drag evaluation at off-design conditions.
($M_1 = 0.726$, $\alpha_1 = 2.44^\circ$)
($M_2 = 0.726$, $\alpha_2 = 2.00^\circ$)
(Markers designate design points.)

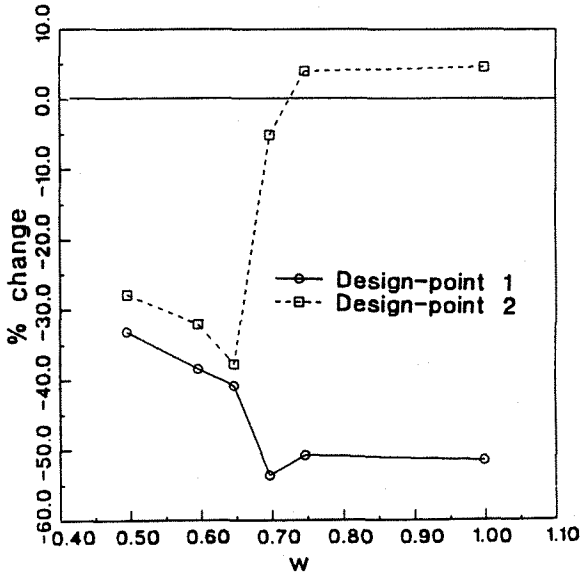

Figure 5. Drag reduction at the two design points versus weighting parameter, w.

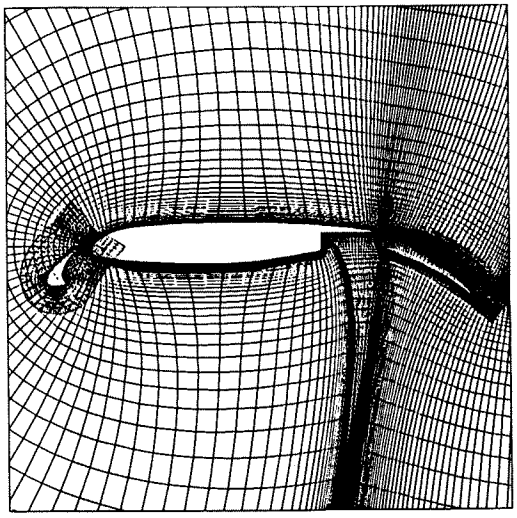

(a) Overall grid

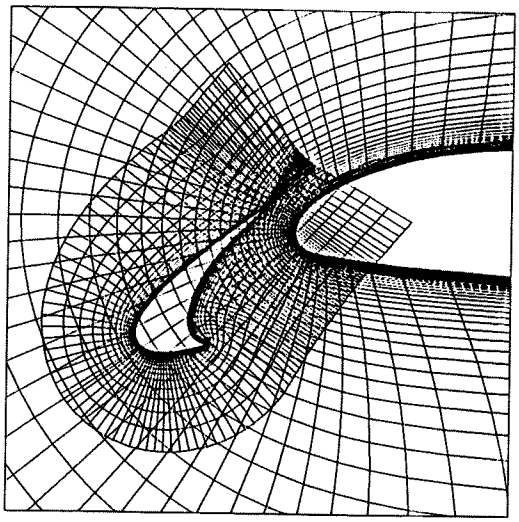

(b) Slat near-field

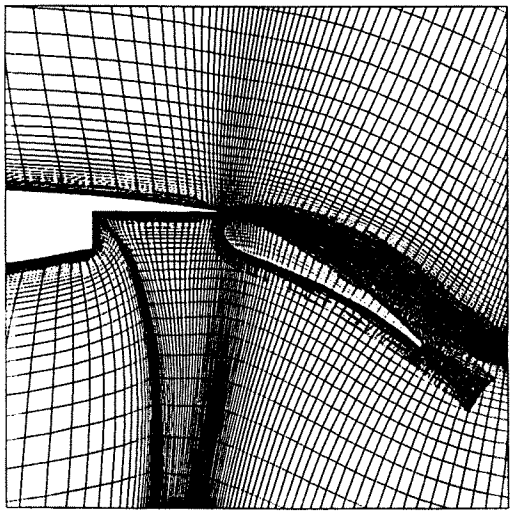

(c) Flap near-field

Figure 6. Grids around a three-element airfoil.

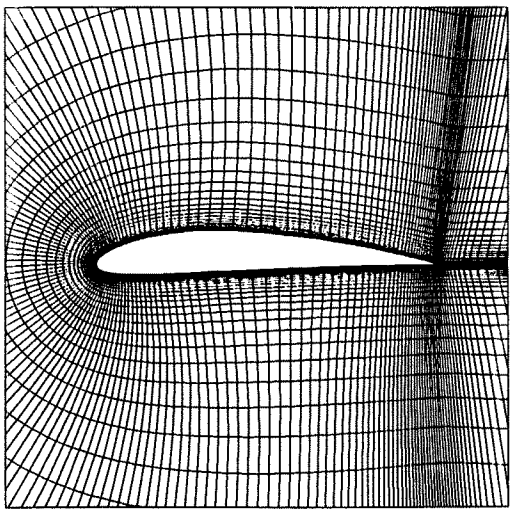

Figure 7. Grid around NACA 4412 airfoil.

Table 2. High-lift design optimization of the NACA 4412 airfoil at $\alpha = 16.0°$.

	Original	Design	Change (%)
C_l	1.701	1.924	13.10
C_d	0.0457	0.0428	–6.30
Area	0.0813	0.0848	4.27

139 function calls, 8330 flow iterations, 37.4 min.

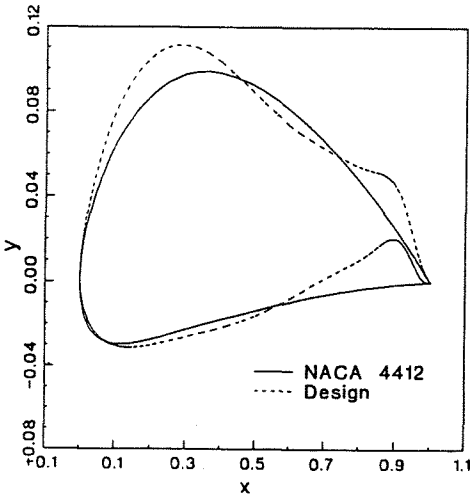

(a) Airfoil geometry

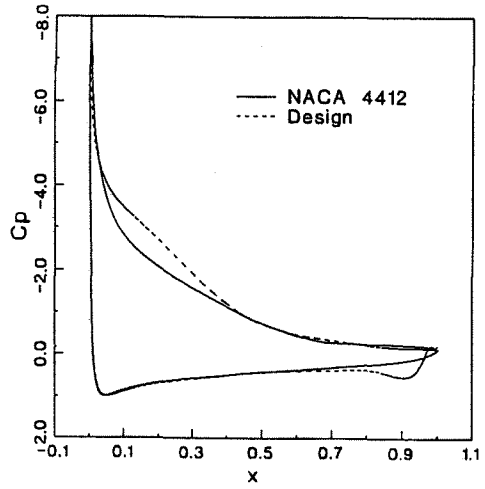

(b) Surface pressure

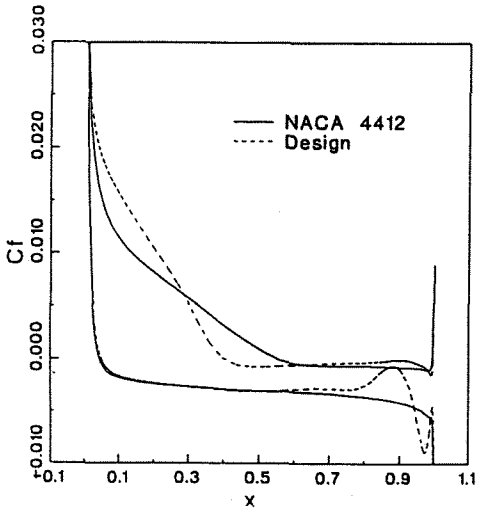

(c) Skin friction

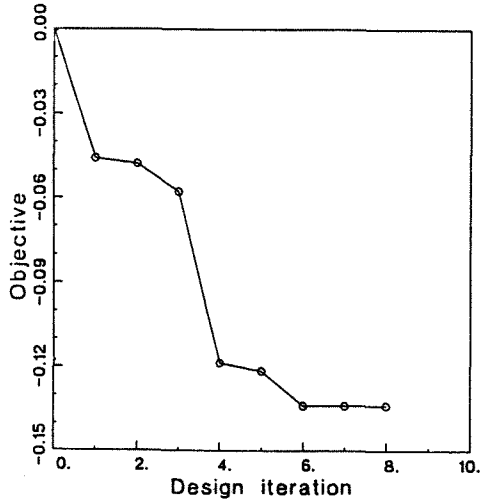

(d) Convergence of objective function

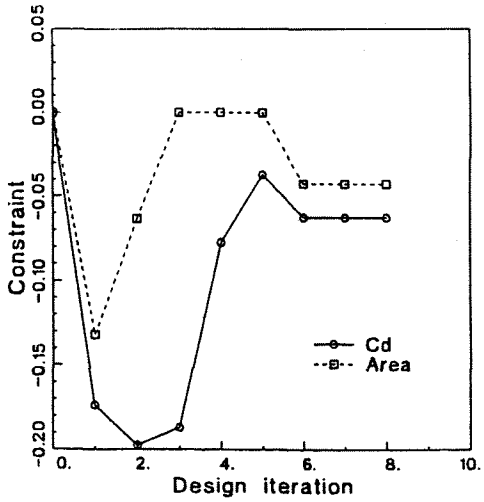

(e) Convergence of constraints

Figure 8. High-lift design optimization of the NACA 4412 airfoil at $\alpha = 16.0°$.

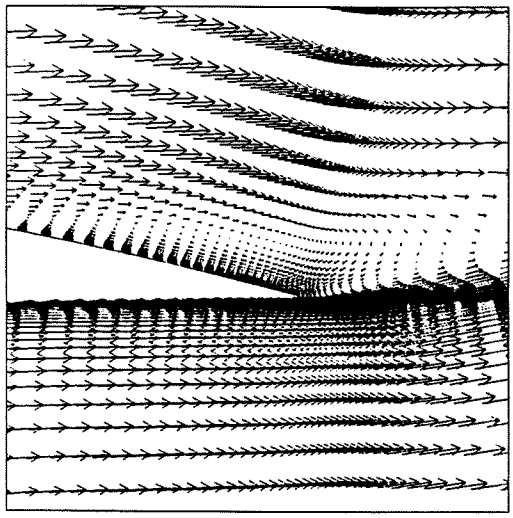

(a) Velocity vectors of NACA 4412

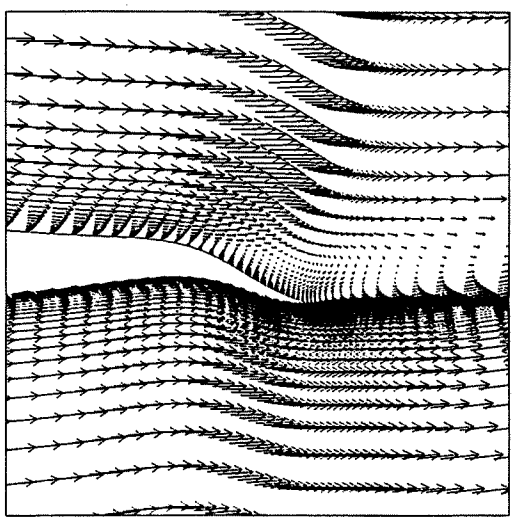

(b) Velocity vectors of designed airfoil

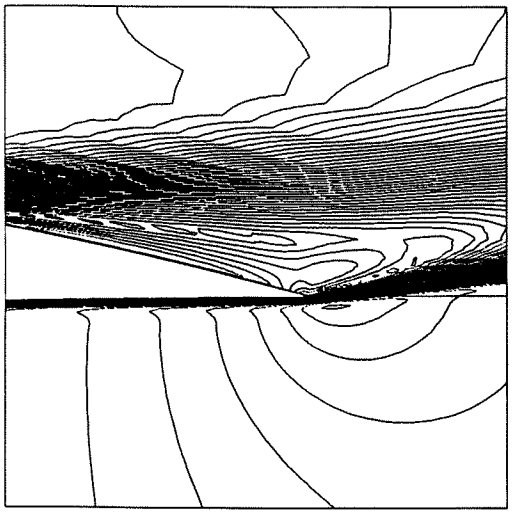

(c) Velocity contours of NACA 4412

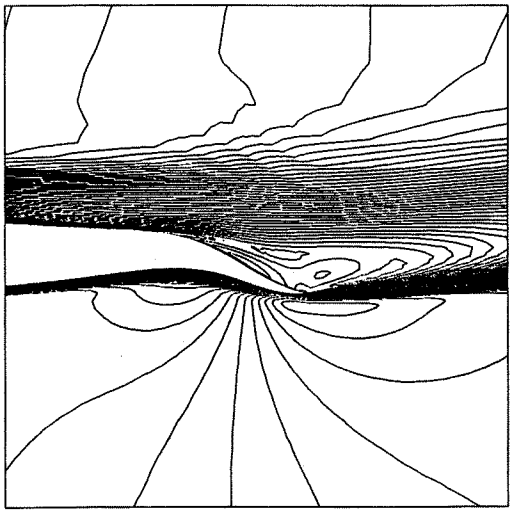

(d) Velocity contours of designed airfoil

Figure 9. High-lift design optimization of the NACA 4412 airfoil at $\alpha = 16.0°$.

Table 3. High-lift design optimization of slat and flap setting for a three-element airfoil.

(a) $\alpha = 8.10°$

	Original	Design	Change (%)
C_l	2.490	2.561	2.84
C_d	0.1035	0.0941	–9.10

21 function calls, 2923 flow iterations, 38.4 min.

(b) $\alpha = 16.21°$

	Original	Design	Change (%)
C_l	3.379	3.515	4.02
C_d	0.1094	0.0961	–12.22

39 function calls, 4327 flow iterations, 56.9 min.

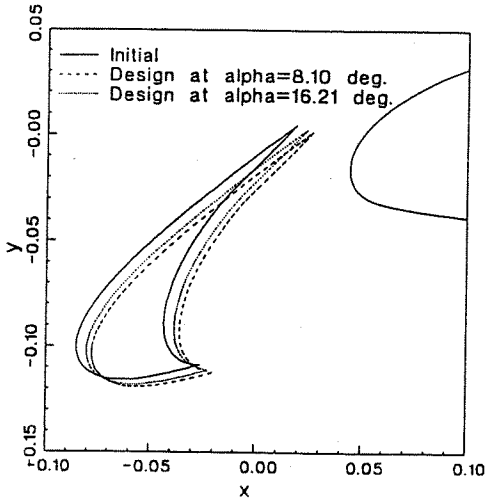

(a) Slat setting

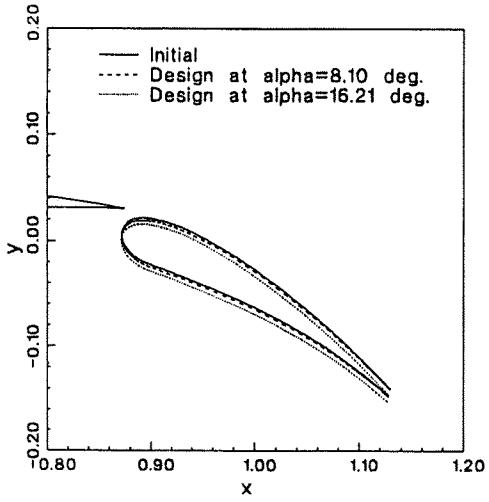

(b) Flap setting

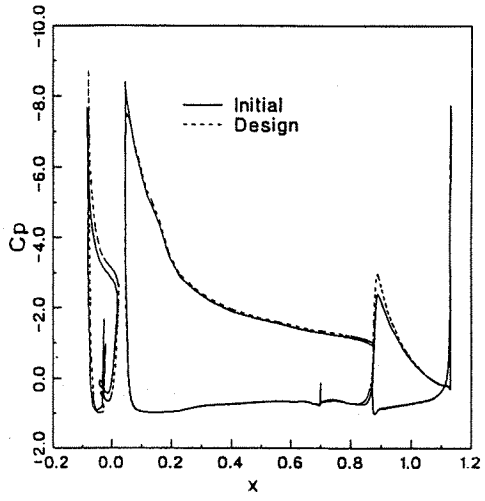

(c) Surface pressure at $\alpha = 16.21°$

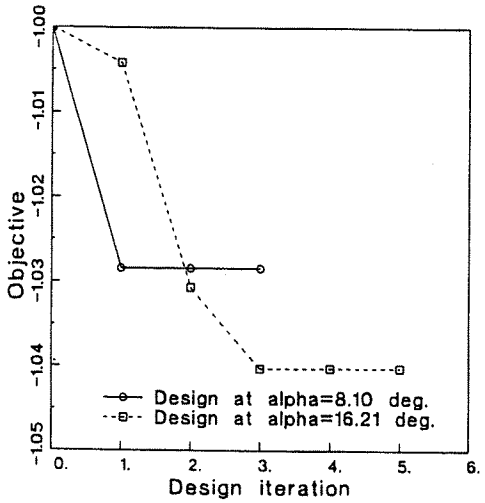

(d) Convergence of objective function

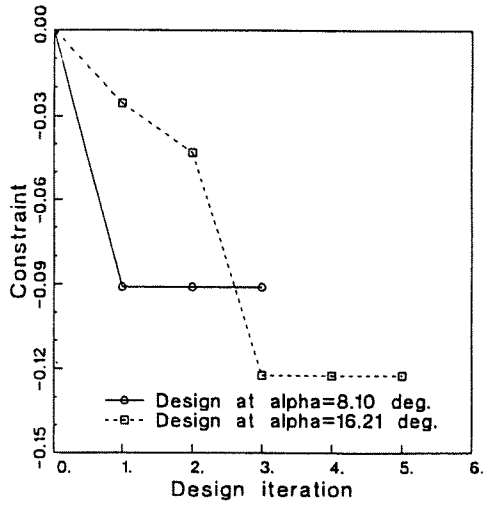

(e) Convergence of constraints

Figure 10. High-lift design optimization of slat and flap setting for a three-element airfoil.